revista Matéria
ISSN 1517-7076
Revista Matéria, v. 15, n. 2, pp. 225–232, 2010.
http://www.materia.coppe.ufrj.br/sarra/artigos/artigo11220

The use of fly-ash and rice-hull-ash in Al/SiCp composites: a comparative study of the corrosion and mechanical behavior

M. I. Pech-Canul[I], R. Escalera-Lozano[II], M. A. Montoya-Dávila[III], M. Pech-Canul[IV]

[I]Cinvestav Saltillo. Carr. Saltillo-Mty Km 13, Saltillo Coah. México 25900.
e-mail: martpech@hotmail.com
[II]Universidad del ISTMO, Campus Tehuantepec. Ciudad Universitaria S/N, Barrio Santa Cruz, 4a. Sección Sto. Domingo Tehuantepec, Oax., México C.P. 70760.
e-mail: miguel.montoya@cinvestav.edu.mx
[III]Cinvestav Mérida. Km. 6 Antigua Carr. a Progreso Apdo. Postal 73, Cordemex. Mérida, Yuc., México 97310.
[IV]Universidad Autónoma de Zacatecas, Carretera a la Bufa km 1, Zacatecas, Zac. México 98064.
e-mail: martin.pech@cinvestav.edu.mx

ABSTRACT

The corrosion characteristics and mechanical behavior of Al/SiCp/spinel composites prepared by reactive infiltration with fly-ash (FA) and rice-hull ash (RHA) -both with recycled aluminum- were investigated. $MgAl_2O_4$ is formed in situ during infiltration in the temperature range 1050-1150 °C for 50-70 min in argon atmosphere at a pressure slightly above to that of the atmospheric pressure. Results reveal that both FA and RHA help in preventing SiC_p dissolution and the subsequent formation of the unwanted Al_4C_3. However, FA-composites are susceptible to corrosion via formation of Al_4C_3 by the interaction of native carbon in FA with liquid aluminum. The foremost corrosion mechanism in both types of composites is attributed to microgalvanic coupling between the intermetallic Mg_2Si and the matrix. Microstructure and mechanical characterization show that FA- and RHA-composites possess mechanical properties that are significantly different and that this behavior is due to the original ash and $MgAl_2O_4$ morphologies. While RHA composites exhibit higher surface hardness than FA composites, the latter display a higher modulus of rupture.

Keywords: Al/SiCp composites; fly ash; rice hull ash.

1 INTRODUCTION

Owing to inherent materials characteristics and post-processing complications –such as corrosion phenomena- the development of metal matrix composites (MMCs) from recycling/waste sources might be a challenging task. Fly-ash (FA) and rice-hull-ash (RHA) are two primary waste materials that offer excellent opportunities for the development of Al matrix composites. Due to its singular shape and low density, FA has attracted the attention of many researchers. For this reason, most of the efforts to develop Al-based composites from waste materials have been centered on the use of fly ash. Extensive research efforts in the use of FA for Al-based composites have been undertaken by Rohatgi and co-workers [1-4]. In addition to lowering costs, incorporation of fly ash into aluminum has been proved to decrease the materials' density, increase their hardness, abrasion resistance and stiffness [1]. One of the major outcomes from the mechanical evaluation of aluminum composites prepared with fly ash is that related to their compression characteristics. Typical compressive stress-strain curves form A356/hollow fly ash composites show a linear elastic region followed by a plateau (associated to the collapse of the hollow particles), and then an increase in stress, representing densification of the foam. The crushing of the cenospheres in the composites has been related to an enhancement in the energy absorption capabilities of the material and to a better damage tolerance [4]. Consideration of rice hull ashes for aluminum-based composites might be of great interest not only because SiO_2 is one of its major constituents like in fly ash, but also because the morphology of rice hull ashes is significantly different from that of FA and therefore different kinds of properties could be obtained.

It has been recognized that special matrix alloys need to be developed to maximize the advantages of fly ash additions [1]. In many respects recycled aluminum may represent a response to this need, particularly to the processing of Al/SiC_p (where the suffix p stands for particulate SiC) composites by the

Autor Responsável: Martin Pech-Canul Data de envio: 25/03/2010 Data de aceite: 23/06/2010

route with the liquid metal. Essentially this is because certain key elements like magnesium (which is essential for pressureless infiltration) would not be required to be eliminated from the alloy, as in the current practice for alloy fabrication from recycled aluminum [5].

In this work, aluminum-based composites were processed by reactive infiltration, starting from SiC_p/FA and SiC_p/RHA porous preforms and two purpose-designed Al-Si-Mg alloys prepared from recycling aluminum. The objective of this investigation was to compare the corrosion and mechanical behavior of FA and RHA composites processed under various conditions and exposed to indoor laboratory atmosphere.

2 EXPERIMENTAL

The aluminum alloys were fabricated in an induction furnace from aluminum beverage containers with additions of commercial Si and Mg. The chemical compositions of the recycling aluminum and the fabricated alloys are shown in Table 1. The alloy Al-8Si-15Mg (wt. %), corresponding to a Si/(Si+Mg) molar ratio of 0.32 was used in the fabrication of generation I composites, and the alloy Al-3 Si-15 Mg (wt. %) with a molar ratio of 0.148, was used in the fabrication of generation II composites. Accordingly, generation I composites prepared with FA are labeled I-FA while those prepared with RHA are designated as I-RHA. The same nomenclature applies for generation II composites, being II-FA and II-RHA, respectively.

Table 1: Chemical composition of recycling aluminum and the fabricated alloys (wt. %)

	Recycled aluminum		**Fabricated alloys**	
	For generation I composites	For generation II composites	For generation I composites	For generation II composites
Si	0.18	0.20	8.37	3.30
Mg	0.61	1.09	15.36	15.58
Fe	0.61	1.43	0.43	1.24
Cu	0.14	0.16	0.11	0.17
Mn	0.84	0.86	0.72	0.65
Others	0.08	0.10	0.15	0.16
Al	Balance	Balance	Balance	Balance

For preparation of the preforms, α-SiC powders with average particle size of 75 μm were thoroughly mixed with fly ash (average particle size ≈ 90 μm) or rice hull ash (average particle size ≈ 100 μm) in a volume ratio of 30:20 (SiC:FA or SiC:RHA) with additions of 8 wt. % dextrin and approximately 0.5 ml of distilled water. Figures 1 (a) and (b) are photomicrographs showing the typical morphologies of FA and RHA, respectively.

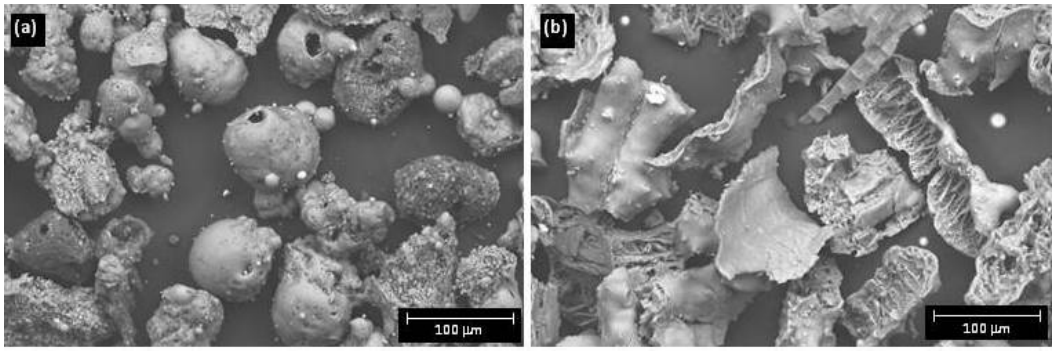

Figure 1: SEM micrographs showing the typical morphology of: (a) fly-ash and (b) rice-hull-ash.

RHA has the appearance of fiber-reinforced flakes while FA has the morphology of hollow spheres, some of them with manifest pores. For fabrication of generation I composites fly-ash was used in the as-received condition and for generation II composites, it was calcined at 900 °C for 30 min; as shown in Table

2, this thermal treatment lowered the carbon content from 1.91 to 0.08 % wt. %. Rice-hull-ash was obtained by calcination of rice hulls at 900 °C for 2 hours under oxidizing atmosphere and used in the as-calcined condition in both generations of composites, I and II. The chemical composition of RHA is also shown in Table 2.

Table 2: Chemical composition of fly ash (FA) and rice hull ash (RHA), (wt. %). FA: Fly ash in the as-received condition, CFA: Calcined fly ash at 900 ^{o}C for 30 min.

	SiO_2	Al_2O_3	MnO_2	Na_2O	K_2O	CaO	Fe_2O_3	TiO_2	MgO	Others	C
RHA	98.5	--	0.12	---	0.29	0.29	0.16	--	0.29	0.35	--
FA	63.95	26.07	0.02	0.02	0.04	2.43	4.88	0.68	--	--	1.91
CFA	67.54	23.75	0.02	0.16	0.21	3.57	4.45	0.22	--	--	0.08

In both cases, the mixed powders were pressed uniaxially into plate-shaped preforms (4 cm x 3 cm x 0.5 cm) with 50 % porosity. Next, the preforms were dried in an air furnace at 125 °C for two hours and then at 225°C for two more hours. The preforms were infiltrated with the corresponding aluminum alloy at three different temperatures (1050, 1100 and 1150°C) for three times (50, 60, and 70 min) using ultra high purity argon at a pressure slightly above to that of the atmospheric pressure (total pressure ≈ 1.2 atm). Infiltration trials were carried out in a horizontal tube furnace provided with end-cap fittings to control the process atmosphere. A K-type thermocouple was used to monitor the specimens' temperature. The preform/alloy sets were placed within ceramic molds and the whole assemblies were positioned at the center of the tube furnace and heated at a rate of 15°C/min up to the test temperature. After completing the established test time, the specimens were cooled down to room temperature at a rate of 15°C/min. Subsequently, the specimens were prepared for evaluation of the apparent density using Archimedes´ principle and for chemical and microstructure characterization by X-ray diffraction (XRD, Cu K_α radiation), scanning electron microscopy (SEM) and energy dispersive X-ray spectroscopy (EDX).

After physical property evaluation and microstructure characterization the composites were exposed to indoor ambient atmosphere. The average relative humidity was 54 %, the minimum ambient temperature was 15 ± 4 ^{o}C and the maximum temperature was 26 ± 5 ^{o}C. Generation I composites exhibited signs of deterioration after one month of exposure, with the appearance of a light-gray powder on its surface. On the other hand, the surface of generation II composites remained free of corrosion products even after one year of exposure. Only specimens having at least 75 % of degree of infiltration were considered for the processing of generation II composites. Generation II composites -which remained uncorroded- from both kinds of ashes were characterized by XRD, SEM/EDX and also evaluated in four-point bending tests and Rockwell superficial hardness tests. The modulus of rupture (MOR) was determined according to the *ASTM C 1161-02c* standard procedures.

3 RESULTS AND DISCUSSION

Results from density measurements indicate that the apparent densities of FA and RHA composites are similar (in the range 2.67 ± 0.08 g cm^{-3}). Likewise, the residual porosity in both types of composites is comparable, with an average of 2.8 ± 1 %.

3.1 Corrosion Behavior

The XRD patterns in Figures 2 (a) and (b) corresponding to I-FA-3 and I-RHA-3 composites (processed both at 1150 °C) reveal that the $MgAl_2O_4$ phase was formed in situ during infiltration. The spinel formation in the composites can be confirmed by contrasting the composites' XRD patterns with the XRD pattern of an alloy like that shown in Figure 2 (c). Figure 2 (c) also shows that the intermetallic Mg_2Si was detected in the characterization of the as-cast aluminum alloy with Si/(Si+Mg) molar ratio equal to 0.32. Evidently, formation of Al_4C_3 in both types of composites was successfully avoided by the presence of FA and RHA in the SiC_p porous preforms. The same result was observed in the other I-FA and I-RHA specimens. The spinel (MgAl2O4) phase in FA- and RHA- composites is formed in accord to reactions (1) and (2).

$$4Al_6Si_2O_{13(s)} + 13\ Mg_{(l)} + 2Al_{(l)} \rightarrow 13MgAl_2O_{4(s)} + 8\ Si_{(in\ l\ Al)} \quad (1a)$$

$$\Delta G_{1100\,^{\circ}C} = -2108 \text{ kJ/mol} \qquad \Delta H_{1100\,^{\circ}C} = -2765 \text{ kJ/mol} \tag{1b}$$

$$4Al_6Si_2O_{13(s)} + 13\,Mg_{(l)} + 2Al_{(l)} \rightarrow 13MgAl_2O_{4(s)} + 8\,Si_{(\text{in } l\text{ Al})} \tag{2a}$$

$$\Delta G_{1100\,^{\circ}C} = -2108 \text{ kJ/mol} \qquad \Delta H_{1100\,^{\circ}C} = -2765 \text{ kJ/mol} \tag{2b}$$

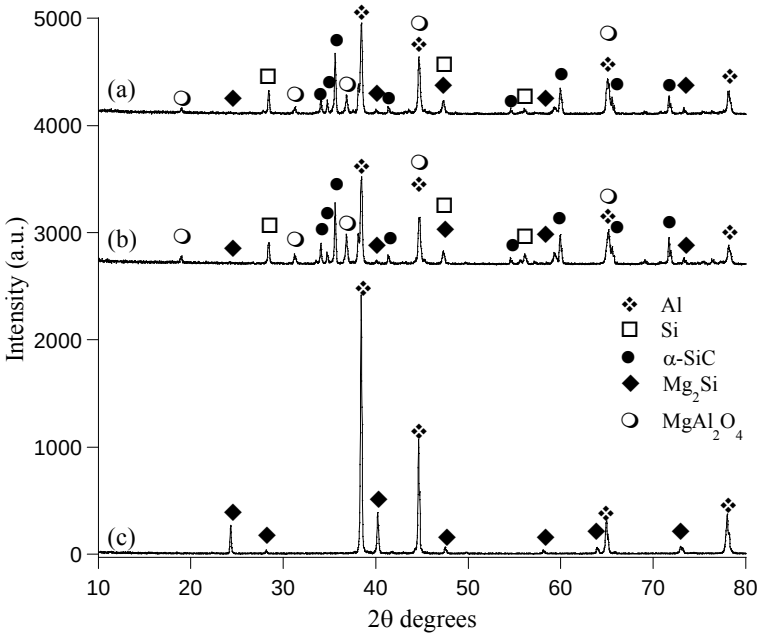

Figure 2: X-ray diffraction patterns of composite specimens: (a) I-FA-3 and (b) I-RHA-3, (c) XRD pattern of the as-cast aluminum alloy with the Si/(Si+Mg) molar ratio 0.32.

Figure 3 (a) exemplifies the typical microstructure of the I-FA composites indicating the round shape of the spinel, due to the fly-ash hollow-spheres. Figure 3 (b) on the other hand, shows the typical microstructure of I-RHA composites.

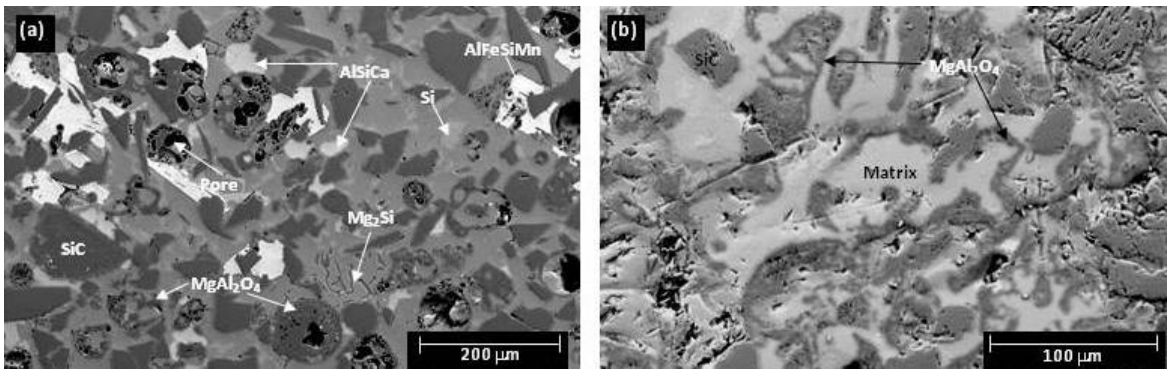

Figure 3: SEM photomicrographs showing the typical microstructure of (a) FA and (b) RHA composites, before exposure to the humid environment.

Thirty days after processing and during exposition to the humid environment, generation I composites from both kinds of ashes manifested signs of degradation, characterized initially by pitting corrosion, followed by the release of white and light-gray powders on the composites surfaces. In FA composites the degradation process was more severe and more rapid because powder release was followed by the formation and propagation of transgranular and intergranular cracks, leading ultimately to a complete disintegration of the composites. In RHA composites however disintegration was only partial. The SEM photomicrographs in Figures 4 (a) and (b) show the microstructure condition of FA and RHA composite specimens during the degradation process, respectively.

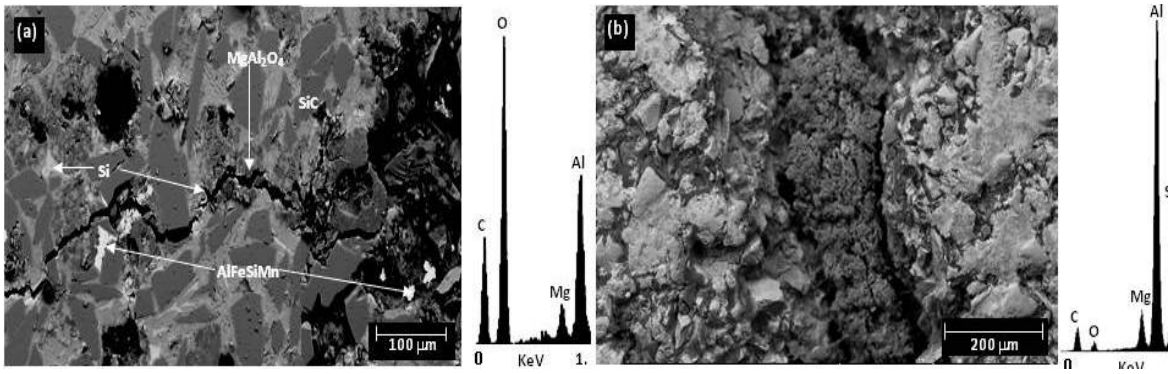

Figure 4: SEM photomicrographs of composite specimens after one month of exposure to the ambient atmosphere: (a) I-FA-3, (b) I-RHA-3.

Regardless of the processing method, several authors [6-8] have shown that in Al/SiC composites the intermetallic Mg_2Si becomes electrochemically active and that behaves as the anode in the galvanic couple. The aggressive damage manifested by the disintegration of the composite into a powdery mixture was most likely due to a galvanic corrosion process where the electrolyte was provided by condensed moisture. Considering the catastrophic nature of the degradation process, the cathode had a large area (compared to that of the anode) and therefore it was most likely comprised by the matrix with possible contribution of the other phases (SiC, Si, $MgAl_2O_4$, AlFeSiMn). More detailed studies with in-situ microelectrochemical techniques would be required to elucidate the relative role of each phase. Figures 4 (a) and (b) also show EDX spectra of degraded regions, revealing the presence of the elements of the spinel, silicon from the alloy and/or that rejected from reactions (1) and (2). The excess of oxygen content was attributed to hydrated aluminum oxide and possibly to the presence of $Mg(OH)_2$.

Figures 5 (a) and (b) show the XRD patterns of loose powders from composites I-FA-3 and I-RHA-3, respectively. In the case of I-FA-3 specimen, in addition to the same phases found in the composite before indoor atmospheric exposure (Figure 3 (a)), the presence of Al_4C_3 was also detected. Although the undesirable Al_4C_3 phase was not detected by XRD in the surface of the FA composites, its presence in the bulk of the composite (and therefore in the loose powders) is quite possible. Regarding the possible origin of such phase, observation that the microstructure condition does not show evidence of considerable attack to the SiC reinforcements by aluminum suggests that Al_4C_3 was not formed by the dissolution of SiC according to equation (3).

$$3SiC_{(s)} + 4\ Al_{(l)} \leftrightarrow Al_4C_{3(s)} + 3\ Si_{(\text{in } l\ \text{Al})} \quad (3)$$

Therefore, aluminum carbide was most likely formed during the infiltration process as a result of the reaction of carbon in the fly ash with the molten aluminum. Conversely, as illustrated in Figure 5 (b) the XRD patterns of loose powders from composites processed with RHA did not reveal the presence of Al_4C_3, showing the existence of exactly the same phases detected in the composites before indoor atmospheric exposure.

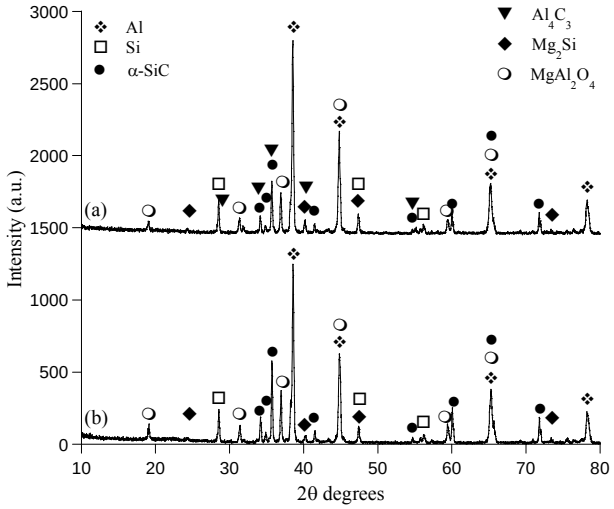

Figure 5: XRD patterns of powdery degradation products formed during composites degradation: (a) I-FA-3, (b) I-RHA-3. The diffractogram in (a) shows the presence of the unwanted aluminum carbide (Al_4C_3) phase.

Figures 6 (a) and (b) are XRD patterns of FA and RHA composites respectively, processed with the alloy Al- 3 Si- 15 Mg (wt. %). Although in the as-cast condition this alloy also exhibited the presence of Mg_2Si, the XRD patterns in Figure 6 suggest that in the composites the alloy-matrix composition is modified in such a way that Mg_2Si is undetected.

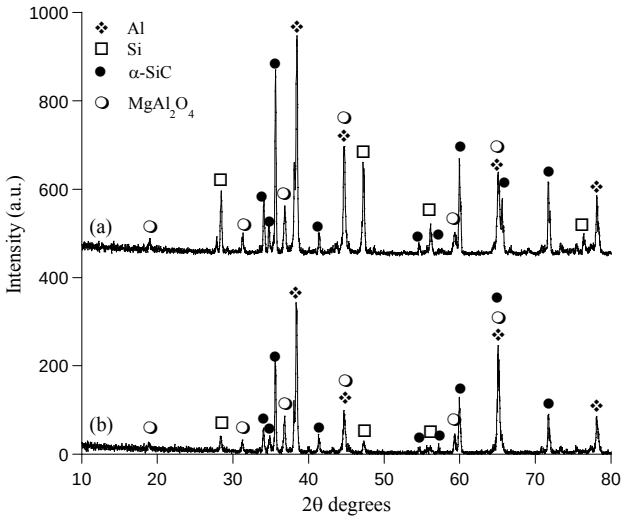

Figure 6: XRD patterns of generation II composites (a) II-FA-3 and (b) II-RHA-3, indicating the absence of Mg_2Si and Al_4C_3.

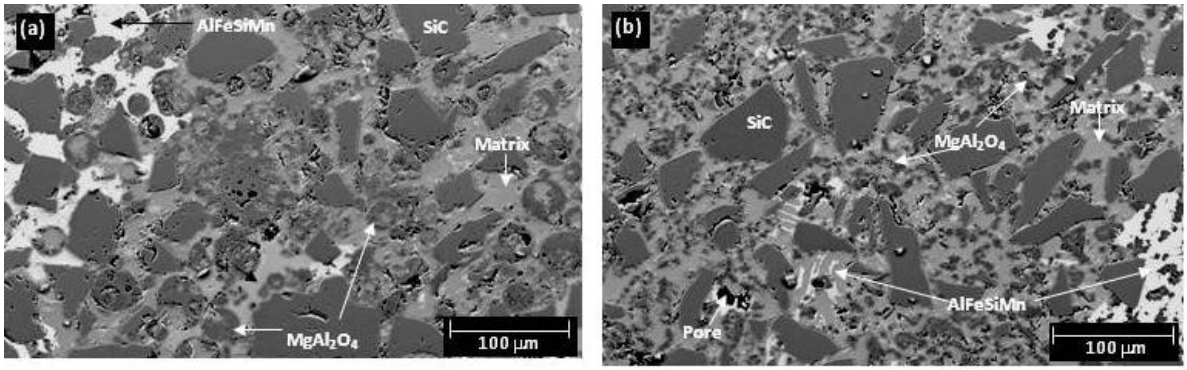

Figure 7: SEM photomicrographs showing the typical microstructure in generation II composites one year after processing: (a) II-FA-3 and (b) II-RHA-3.

The absence of such intermetallic compound explains the physical integrity of the composites even after one year of exposure to the humid environment, because microgalvanic corrosion (the most important degradation mechanism observed for generation I composites) did not take place. Besides, chemical degradation did not happen either, because formation of the Al_4C_3 phase was successfully avoided by the presence of SiO_2 (in FA and RHA added to the SiC_p performs) and by the absence of carbon in the calcined fly ash. The soundness of generation II composites is evidenced through photomicrographs of specimens after one year of exposure to humid environment, as shown in Figure 7.

3.2 Mechanical property evaluation

According to the physical property characterization, discussion on the composites (generation II composites, which remained uncorroded) mechanical properties is made under the assumption that both FA and RHA composites have similar total residual porosity. However, it should be recognized that the origin of such porosity is different. As it is shown in Figure 1, a number of cenospheres have pores through which the liquid aluminum alloy can be incorporated during infiltration. Thus, during the infiltration process some of the spheres in FA specimens are completely filled by liquid aluminum and some of them are just partially filled in. For this reason, FA-composites have two types of porosity, namely, interparticle porosity and cenosphere related porosity. The former occurs by an incomplete or partial infiltration while the latter is due to the unfilled or partially filled cenospheres. Even though the total amount of porosity is similar in both types of composites, the relative contribution of cenosphere related porosity is unknown.

As for the flexural tests, for the most part FA composites exhibited higher modulus of rupture (MOR) than RHA composites. Yet when the difference in the processing conditions does not allow to making a direct comparison in mechanical properties, this result can be explained as follows. Since the interfacial strength is more important in tensile and flexural properties than in compression, it can be reasonably concluded that the better performance exhibited by FA composites is due to the interfacial condition between the spheres and the alloy matrix. However, since in flexural tests the upper face of the specimen is subjected to compressive stresses, the unfilled or partially filled spheres in the vicinity of the compressive domains might experience an effect similar to that observed in fly ash composites under compression. Moreover, the difference between the morphology of the $MgAl_2O_4$ derived from FA and RHA - as it can be seen in the photomicrographs shown in Figure 3 (a) and (b)- might also be an important contributing factor. Because of the spherical morphology of FA and due to the more uniform stress distribution around spheres, FA composites are less susceptible to fail by stress concentration effect than RHA composites. Accordingly, the higher modulus of rupture observed in FA composites can be explained by the confluence of three different factors: i) better stress distribution around the spheres, ii) good interfacial strength between the spheres and the alloy matrix and, iii) enhanced energy absorption capabilities by the crushing of the unfilled or partially filled spheres.

Results from 4-point flexural tests of II-FA composites show that the specimens processed at 1150 ^oC exhibit higher fracture strength than those prepared at 1100 ^oC, being the average MOR values of 185 ± 5 and 138 ± 5 MPa, respectively. This difference can be explained in terms of retained porosity in the composites. Since the liquid metal fluidity increases with increase in temperature, it can be reasonably expected that at 1150 ^oC the cenospheres will be better filled than at 1100 ^oC. Moreover, aluminum incorporation into the spheres is also driven as a consequence of the exothermic reactions between the fly-ash and the liquid aluminum alloy. Although the apparent porosity in the II-FA specimens is similar (≈ 2.8 ± 1 %) at both temperatures, it is suggested that the mechanical response of composites processed at 1100 ^oC is more influenced by cenosphere related pores than that of specimens prepared at 1150 ^oC. That explains why the former exhibit lower fracture strength than the latter. Besides, as illustrated in Figures 3 (a) and 7 (a), in composites from both generations (I-FA and II-FA), interparticle porosity is less significant than cenosphere porosity. Figure 11 gives evidence of the extent of porosity left behind by an incomplete filling of aluminum through the cenosphere pores.

The Rockwell hardness tests showed that RHA composites have a higher hardness than their FA counterparts. Again, this result might be associated to the morphology of the spinel resulting from the rice hull ashes. Besides it can be expected that the composites' hardness will be influenced by the ash origin and the relative amount of in situ phases formed. As far as morphology is concerned, the spinel derived from RHA roughly keeps the same morphology of the rice hull ash, which has the appearance of fiber-reinforced flakes. On the other hand, since RHA has about 50 % more silica than fly-ash, it would be expected that the RHA composites have a higher proportion of $MgAl_2O_4$ than FA composites. However, results from the semi-quantitative phase analysis from the XRD patterns showed that the difference in spinel content is irrelevant. In this context, it can be concluded that the difference in both superficial hardness and MOR is more dominated by the morphology of the in situ formed spinel than by its content (see Table 3).

Table 3: Average mechanical properties of FA and RHA composites

Composite type	Rockwell Superficial hardness	MOR (MPa)
II-FA	28.19 ± 2.8	185 ± 4.6
II-RHA	41.38 ± 3.1	109 ± 3.5

4 SUMMARY AND CONCLUSIONS

For generation I composites prepared with the alloy Al-8Si-15Mg (wt. %), corresponding to a Si/(Si+Mg) molar ratio of 0.32, the intermetallic Mg_2Si is responsible for the catastrophic localized corrosion observed in the presence of condensed humidity because it acted as a microanode coupled to the matrix. Although the potential attack of SiC by liquid aluminum was successfully avoided by the presence of SiO_2 (in the FA and RHA added to the SiC_p performs) in FA composites Al_4C_3 was still formed due to the reaction of carbon in the fly ash with aluminum. So, chemical degradation also took place. The Al_4C_3 formed by carbon in FA and liquid aluminum accelerates the degradation process and leads to a more aggressive damage. For generation II composites, processed with the alloy Al- 3Si- 15 Mg (wt. %) the silicon content was low enough to avoid the formation of Mg_2Si. The absence of such intermetallic compound explains the physical integrity of the composites even after one year of exposure to the humid environment. Moreover, in both types of composites chemical degradation did not happen either, because formation of the Al_4C_3 phase was successfully avoided by the presence of SiO_2 and by the elimination of carbon in fly ash. Results from the mechanical property evaluation show that FA composites exhibit a higher MOR than their RHA counterparts but that the latter exhibit a higher superficial hardness than the former. Moreover, the lower MOR exhibited by FA composites processed at low temperature is explained by higher level of cenosphere related porosity. The difference in the mechanical response of both types of composites is attributed to the morphology of the original ash and to that of the in situ formed spinel.

5 REFERENCES

[1] ROHATGI, P.K., "Low-cost, Fly-Ash-Containing Aluminum-Matrix Composites", *JOM - The Member Journal of TMS*, v. 46, n. 11, pp. 55-59, 1994.

[2] GUO R.Q., VENUGOPALAN, D., ROHATGI, P.K., "Differential thermal analysis to establish the stability of aluminum-fly ash composites during synthesis and reheating", *Materials Science Engineering A*, v. A241, pp. 184-190, 1998.

[3] ROHATGI P.K., GUO, R.Q., IKSAN, H., BORCHELT, E.J., ASTHANA, R., "Pressure infiltration technique for synthesis of aluminum-fly ash particulate composites", *Materials Science Engineering A*, v. A244, pp. 22-30, 1998.

[4] ROHATGI, P.K., KIM, J.K., GUPTA, N., ALARAJ, S., DAOUD, A., "Compressive characteristics of A356/fly ash cenosphere composites synthesized by pressure infiltration technique", *Composites* Part A, v. 37, pp. 430-437, 2006.

[5] MACIAS-AVILA, E, FLORES-VALDÉS, A, "A kinetic model for removal of magnesium from molten aluminum by Na_2SiF_6 submerged powder injection", *Aluminum Transactions*, v. 1, n. 1, pp. 79-92, 1999.

[6] NUNES, P.C.R., RAMANATHAN, L.V., "Corrosion behavior of alumina-aluminum and silicon carbide-aluminum metal-matrix composites", *Corrosion*, v. 51, n. 8, pp. 610-617, 1995.

[7] ANDREATTA, F., TERRYN, H., WIT, J.H.W., "Effect of solution heat treatment on galvanic coupling between intermetallics and matrix in AA7075-T6", *Corrosion Science*, v. 45, pp. 1733-1746, 2003.

[8] CANDAN, S., BILGIC, E., "Corrosion behavior of Al-60 vol. % SiC_p composites in NaCl solution", *Materials letters*, v. 58, pp. 2787-2790, 2004.